Re-evaluation of the Hiroshima Hypocenter Based on Data in ABCC Technical Reports 12-59 and 3-69: Some Initial Ideas and Results

Harry Cullings*, Shoichiro Fujita
Radiation Effects Research Foundation
Masaharu Hoshi
Hiroshima University

Abstract
Modern software and associated computing speed allow a better evaluation of data on the hypocenter than was feasible even ten years ago. Hubbell, Jones, and Cheka wrote a report in 1969, ABCC Technical Report 3-69, which is the source of the Hiroshima hypocenter estimate used in the DS86 and DS02 dosimetry systems. They made an exhaustive study of all available data at that time and they documented all of the available data explicitly in their report, except for data that were documented previously in an earlier report, ABCC TR 12-59. For the present work all of these data were entered into spreadsheets. In addition to direct entry of tabular numerical data, data implicit in maps and drawings were obtained in numerical form by using the Geographical Information System (GIS) to locate them in the map coordinate systems used in DS02. The GIS was also used to check 1) the coordinates of measured locations whose identity is established by site names or other such information, 2) various hypocenter estimates of the original studies as drawn on maps and figures by the original investigators, and 3) various hypocenter estimates of the original studies as given by the original investigators in reference to landmarks of known location. Measurement locations could be checked against aerial photographs and modern maps using the GIS, with correction if appropriate, and estimates of hypocenter location specified above in (2) and (3) could be evaluated in the GIS and compared to numerical coordinate values given by the original investigators or cited from other sources in ABCC TR 3-69. The raw data from four major studies on which the Hiroshima hypocenter estimate of TR 3-69 was primarily based (Kimura and Tajima, Arakawa and Nagaoka, Kanai, Woodbury and Mizuki), were extensively analyzed. The least-squares fitting method given by Arakawa and Nagaoka in TR 12-59 was augmented to allow for specification of the penumbra effect from a fireball of any specified size, and combinatorial methods were used to check the effects of various related assumptions on the results of the two major studies (Arakawa and Nagaoka, Kanai) in which the authors did not explicitly treat the penumbra issue nor document the sides of the shadow-casting objects on which they took measurements. A new uncertainty analysis was performed, including the definition of a new statistic similar to the one used in TR 3-69, to provide a way to relate the information in the data themselves (how close the measured rays come to intersecting at a single, common point) to the uncertainty in the input variables (X and Y coordinates of measured locations, angles measured) and the resulting uncertainty in the corresponding hypocenter estimate. This relationship was elucidated and estimated by numerical simulations of random errors, including the simulation of many plausible sets of measurement locations for studies for which the measurement locations are not available. A new weighting scheme similar to that suggested by Land in TR 3-69 was devised and used to obtain a new hypocenter estimate. In contrast to the work of DS02, which used a map alignment to define the location in new city map coordinates of the hypocenter determined in U.S. Army map coordinates by Hubbell, Jones, and Cheka, this more

* Harry CULLINGS, Radiation Effects Research Foundation; hcull@rerf.or.jp

fundamental work completely re-analyzes the data used by Hubbell, Jones, and Cheka. Initial indications are that the new estimate may be about 17 m south of their estimate.

Introduction

For almost 20 years, dosimetry working groups (RERF 1987) have used an estimate of the atomic bomb hypocenter location in Hiroshima that was produced in 1969 by a thorough review of earlier studies. This review was conducted by scientists of the U.S. Oak Ridge National Laboratory and published in an ABCC (Atomic Bomb Casualty Commission) Technical Report, No. 3-69 (Hubbell et al. 1969). A major strength of ABCC TR 3-69 is that it did an excellent job of preserving all of the detailed information that was available in 1969 from earlier studies. ABCC TR 3-69 and an earlier ABCC report produced in 1959, No. 12-59 (Arakawa and Nagaoka 1959, Woodbury and Mizuki 1959), taken together, contain all of the raw data, consisting of measurement locations and measured angles to the hypocenter at those locations, for four major studies that were the main basis of the estimate produced in ABCC TR 3-69. Although the joint binational working group that prepared the DS02 dosimetry system conducted a major reanalysis of map issues using modern Geographical Information System (GIS) software, time and resource constraints compelled them to use the hypocenter estimate of 1969, as originally defined on the 1945 U.S. Army map of Hiroshima, for which they determined a new estimate of the corresponding location on new city maps produced by the City of Hiroshima in 1979. This transfer of the ABCC TR 3-69 hypocenter to more modern maps was based strictly on the alignment of the two sets of maps. That is, DS02 did not attempt to re-analyze the original raw data(Young and Kerr 2004).

The possibility of re-analyzing the raw data of ABCC TR's 12-59 and 3-69 is interesting in the first place because of the great progress in computerized computation and related information systems since the 1960's. Contemporary Geographical Information Systems (GIS's) allow maps and aerial photographs to be combined in ways that enable more accurate estimation of the map coordinates of sites where angles to the hypocenter were measured (Young and Kerr 2004). Modern computer software in the form of spreadsheets and programming languages allows greatly facilitated computation, and the speed of modern computers allows much larger calculations for purposes such as numerical simulation of statistical problems. Furthermore, statistical methods such as linear regression have been extensively developed and elaborated in the last several decades (Draper and Smith 1981).

In addition to the advantages of modern methods and computers, a careful reading of ABCC TR's 12-59 and 3-69 reveals that a number of problems related to analyzing and interpreting the original raw data were never resolved. This paper will focus on solutions to three of the most prominent of those problems:

1. Devising a method to analyze the data of measurers who failed to record the sides of shadow-casting objects on which they made measurements of the angles of the edges of shadows from the bomb's thermal radiation (the penumbra problem),
2. Devising a statistic that uses the information implicit in the measurements of such angles for a given study, and a method of estimating the distribution of that statistic, so that it can be used in turn to estimate the uncertainty of the resulting hypocenter estimate of that study (the measurement uncertainty problem), and
3. Using the uncertainty estimates so derived to construct an appropriate method of statistical weighting to be used in combining the results of the original studies considered in ABCC TR 3-69 (the statistical weighting problem).

We take the solution proposed here for the penumbra problem and apply it to the data of Kanai, which was an unresolved enigma for the authors of ABCC TR 3-69. We take the solution proposed for the

measurement uncertainty problem and illustrate it using the data of Arakawa and Nagaoka (Arakawa and Nagaoka 1959), which consist of 1178 total measurements at 37 different sites and represent by far the largest recorded data set of the four major studies used in ABCC TR 3-69. In both of these cases we also give the results of using the GIS to re-evaluate the coordinates of the sites where the measurements were made. Finally, we use the solution to the third problem to combine the resulting estimates of the hypocenter location from the data of Kanai and those of Arakawa and Nagaoka with similarly derived estimates for the other studies considered in ABCC TR 3-69, to produce a new initial estimate of the hypocenter location.

Methods

The Penumbra Problem

Data collected by measuring shadows created by the thermal radiation from the bomb comprise almost all of the information on which the authors of ABCC TR 3-69, and most reports cited by them, based their estimates of the location of the Hiroshima hypocenter. The source of thermal radiation, which is identifiable with the "fireball," was substantial in size, a fact remarked upon repeatedly by Hubbell, Jones and Cheka in ABCC TR 3-69. As a result, shadows preserved by the alteration of surfaces by the thermal radiation from the fireball had a penumbra, as shown in Figure 1. Because investigators naturally tried to measure the outer edge of the penumbra, where it blends into the area of no shadow, they measured the angle to one side of the fireball that constitutes the source of radiation producing the shadow, and not the center of the source. A measurement on one side of the shadow-casting object corresponds to one side of the fireball, and a measurement on the other side of the object corresponds to the other side of the fireball.

The investigators performing two of the major studies considered in ABCC TR 3-69 (Kimura and Tajima, Woodbury and Mizuki) measured shadows on both sides of an object and took a ray halfway

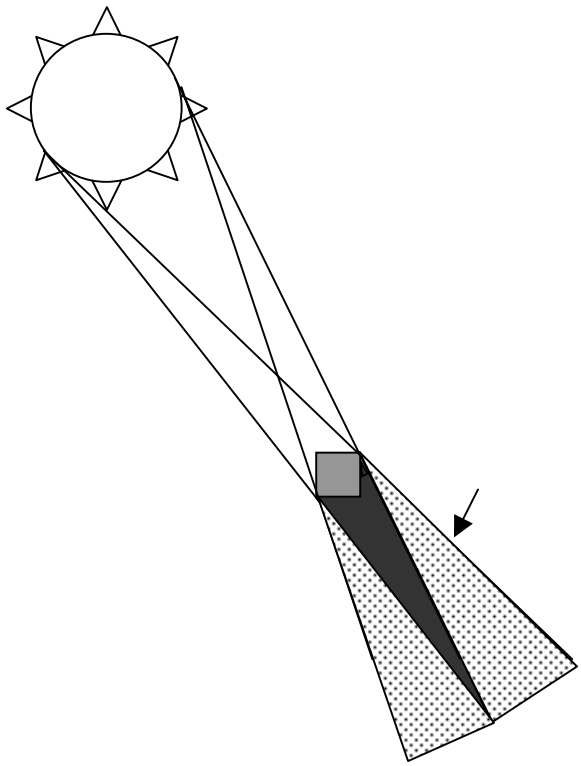

Figure 1. Shadows from a source of non-negligible extent create an area of partial shadow, the penumbra, adjacent to the full shadow, or umbra

between the rays so measured as being a ray to the center of the fireball. However, in the other two major studies (Kanai, Arakawa and Nagaoka), there is no information in ABCC TR 12-59 or ABCC TR 3-69 about which sides of the shadow-casting objects were measured, nor is there information to establish whether or not a procedure to obtain a central ray was followed. Treatment of the penumbra in two of the four major original studies was therefore a problematic issue in the writing of ABCC TR 3-69 and has remained an unresolved question to the present day.

To attack this problem we began by choosing the method of solving for a hypocenter estimate that was originally proposed by Arakawa and Nagaoka in Part I of ABCC TR 12-59, and appears to give good results. (That is, the solutions obtained by this method, unlike the solutions obtained by the methods suggested by Woodbury and Mizuki in Part II of ABCC TR 12-59, appear by visual inspection of plots to be central to the measured rays. This issue will be documented further in future work.) We follow the authors' original nomenclature, which is illustrated in Figure 2, taken from their work (Arakawa and Nagaoka 1959). That is, (x,y) are the coordinates of the hypocenter, (x_i,y_i) are the coordinates of the location where the i^{th} measurement was made, the measured azimuthal angle α_i is specified counter-clockwise from grid east, and d_i is the perpendicular (and shortest) distance from the ray to the hypocenter. Based on the simple but elegant geometry that Arakawa and Nagaoka illustrated in Fig. 2, they observed that

$$d_i = AB - AC = (y - y_i)\cos\alpha_i - (x - x_i)\sin\alpha_i \quad (1)$$

(i.e., ABxy and ACx_iy_i are similar right triangles, so that the length of segment AC is given by $\sin\alpha_i = AC/Ax_iy_i = AC/(x - x_i)$, where we have used "$Ax_iy_i$" to denote the length of the segment from the point labeled A to (x_i,y_i), etc.). They suggested finding a hypocenter estimate (x,y) that minimizes the weighted sum of squares of the d_i, which they denoted as Λ, by setting the first derivatives equal to zero, i.e.,

$$\Lambda = \sum_{i=1}^{m} n_i d_i^2, \quad -\frac{1}{2}\frac{\partial\Lambda}{\partial x} = \sum_{i=1}^{m} n_i d_i \sin\alpha_i = 0, \quad \frac{1}{2}\frac{\partial\Lambda}{\partial y} = \sum_{i=1}^{m} n_i d_i \cos\alpha_i = 0 \quad (2).$$

FIGURE 5 PROCEDURE USED FOR CALCULATING LOCATION OF THE HYPOCENTER
図5 爆心地点の計算に用いられた方法

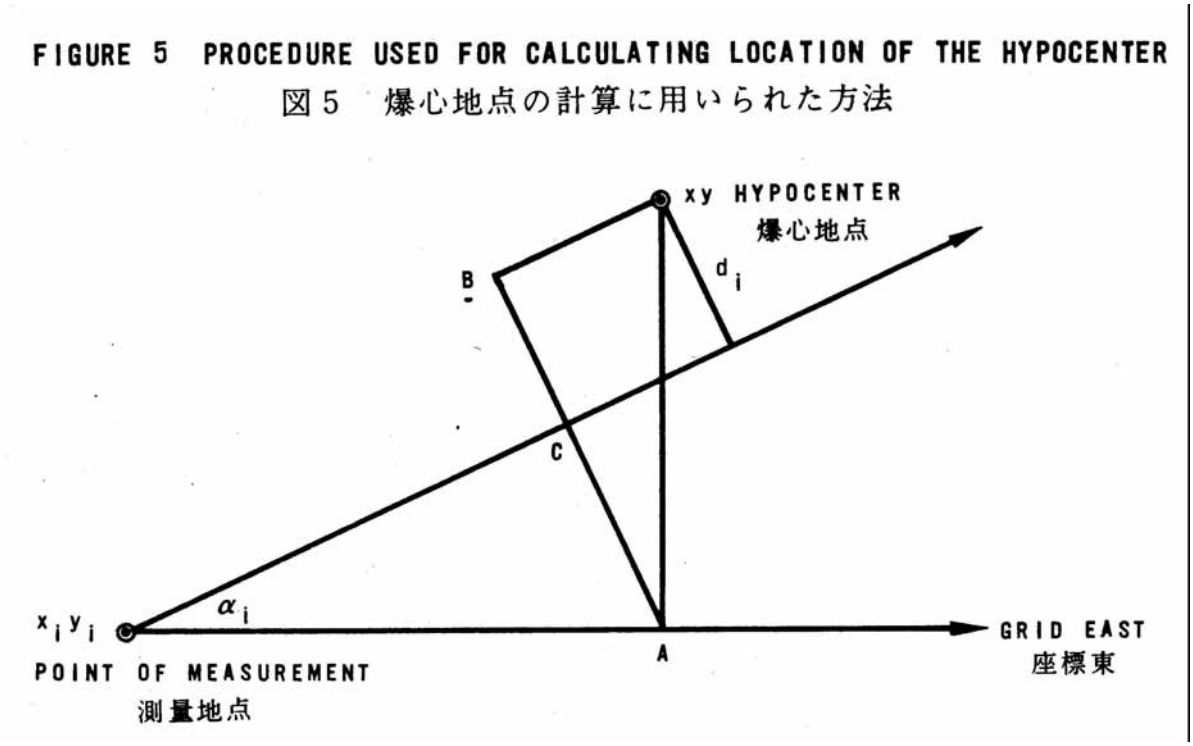

Figure 2. Notation for measurements parameterized as X-Y coordinates of the measurement location and azimuthal angle (reproduced from Arakawa and Nagaoka (Arakawa and Nagaoka 1959)

Here m is the number of measured locations, n_i is the number of measurements at the i^{th} location, and the weighting reflects the presumed dependence of the variance of, e.g., the mean of n measurements, on n.
With some additional algebra (shown below for the case in which we assume a fireball of some fixed radius), this results in a solution

$$x = \frac{C(P-R) - B(Q-S)}{AC - B^2},\ y = \frac{B(P-R) - A(Q-S)}{AC - B^2} \quad (3),$$

where

$$A = \sum_{i=1}^{m} n_i \sin^2 \alpha_i,\ B = \sum_{i=1}^{m} n_i \sin \alpha_i \cos \alpha_i,\ C = \sum_{i=1}^{m} n_i \cos^2 \alpha_i,\ P = \sum_{i=1}^{m} n_i x_i \sin^2 \alpha_i,$$

$$Q = \sum_{i=1}^{m} n_i x_i \sin \alpha_i \cos \alpha_i,\ R = \sum_{i=1}^{m} n_i y_i \sin \alpha_i \cos \alpha_i,\ and\ S = \sum_{i=1}^{m} n_i y_i \cos^2 \alpha_i \quad (4).$$

It is easy to rewrite and solve the equations of Arakawa and Nagaoka for optimization to a circle of some fixed radius r about the hypocenter. In that case we do not want the d_i to be as small as possible, but rather as close as possible to some specified effective fireball radius r. Using the same notation, we write

$$\Lambda = \sum n_i (d_i - r)^2 = \sum n_i [(y - y_i)\cos \alpha_i - (x - x_i)\sin \alpha_i \pm r]^2 \qquad (15)$$

wherein the sign of the term for r depends on which side of the shadow-casting object was measured, as discussed further below. (Consistent with the notation of Arakawa and Nagaoka, we have omitted the limits on the summations for simplicity; they are all "i = 1 to m.")
Then taking the first partial derivatives with respect to x and y gives

$$\frac{\partial \Lambda}{\partial x} = -2\sum n_i [(y - y_i)\cos \alpha_i - (x - x_i)\sin \alpha_i \pm r]\sin \alpha_i$$

$$\frac{\partial \Lambda}{\partial y} = -2\sum n_i [(y - y_i)\cos \alpha_i - (x - x_i)\sin \alpha_i \pm r]\cos \alpha_i \qquad (16),$$

and setting them equal to zero gives

$$\sum n_i (\hat{y} - y_i)\sin \alpha_i \cos \alpha_i = \sum n_i (\hat{x} - x_i)\sin^2 \alpha_i + \sum \pm n_i r \sin \alpha_i$$

$$\sum n_i (\hat{y} - y_i)\sin \alpha_i \cos \alpha_i = \sum n_i (\hat{x} - x_i)\sin^2 \alpha_i + \sum \pm n_i r \cos \alpha_i \qquad (17)$$

which expand to

$$\hat{x}\sum n_i \sin^2 \alpha_i - \hat{y}\sum n_i \sin \alpha_i \cos \alpha_i = \sum n_i x_i \sin^2 \alpha_i - \sum n_i y_i \sin \alpha_i \cos \alpha_i - \sum \pm n_i r \sin \alpha_i$$

$$\hat{x}\sum n_i \sin^2 \alpha_i - \hat{y}\sum n_i \sin \alpha_i \cos \alpha_i = \sum n_i x_i \sin^2 \alpha_i - \sum n_i y_i \sin \alpha_i \cos \alpha_i - \sum \pm n_i r \cos \alpha_i$$

(18).

Abbreviating the summations for the remaining algebra, we can write

$$A\hat{x} - B\hat{y} = P - R - T$$

$$B\hat{x} - C\hat{y} = Q - S - U \qquad (19),$$

from which

$$\hat{x} = \frac{P - R - T + By}{A} = \frac{C(P - R - T) + B^2 \hat{x} - B(Q - S - U)}{AC} \Rightarrow$$

$$\hat{x} = \frac{1}{1 - \frac{B^2}{AC}}\left(\frac{C(P - R - T) - B(Q - S - U)}{AC}\right) = \frac{AC}{AC - B^2}\left(\frac{C(P - R - T) - B(Q - S - U)}{AC}\right)$$

$$= \frac{C(P - R - T) - B(Q - S - U)}{AC - B^2} \qquad (20).$$

Similarly,

$$\hat{y} = \frac{B(P - R - T) - A(Q - S - U)}{AC - B^2} \qquad (21),$$

wherein we have kept A through S exactly as defined by Arakawa and Nagaoka, and we have added the expressions T and U, in which we must remember that the signs of the individual terms depend on which side of the shadow-casting object was measured. The correct sign is obtained by the rule that, if the angle is measured counterclockwise from due E, reverse (to negative) the signs for terms corresponding to a ray that is drawn to the left side of the fireball, i.e., the ray with the larger angle of the two to either side of the fireball. Looking *away* from the hypocenter *toward* the point of measurement, this is the shadow on the *left* side of the structure casting the shadow: the side indicated by the arrow in Fig. 1.

When only one of two rays has been measured, and one knows not which, the problem is to decide which sign to associate with each term in T and U. In the case of only two rays, the correct decision is obvious, because only one solution lies in the correct direction with respect to the directions of the rays. For larger numbers of rays, the correct solution is not necessarily obvious. For a single measurement at each of m locations, there are 2^m possible solutions, defined by changing or not changing the sign of each term in T, where each term in U has the same sign as the corresponding term in T. For numbers of locations around 18 to 20 or so, it is quite feasible to exhaustively check each of these possible combinations to see which one has the smallest residual sum of squared distances between the rays and the circle representing the effective fireball radius. This provides a truly optimal solution in cases lacking the side-measured information, and this method can be used to learn something about the individual data sets, as shown in the following analysis for the data of Kanai.

The method that was devised for exhaustive checking was to

- use the digits of a binary number between 0 and 2^{m+1}-1, including all of the leading zeros to the full width of m characters,
- increment the number from 0 to 2^{m+1}-1 in steps of 1, and
- for each such number, equate the sign of each term with the 1 or 0 of the corresponding digit.

The terms A, B, C, P, Q, R, and S do not have to be recalculated for these combinations, only the terms T and U need be recalculated. In this code, as in the code for numerical simulation of random errors described below, the results of the code for representative sets of input values were extensively cross-checked against spreadsheet calculations of the same solutions to assure correct results.

The situation is illustrated here with a simple example. Figure 3 shows measured rays for both sides of the shadow-casting objects at three hypothetical locations, using the grid coordinates of the newer city map of Hiroshima for illustration. In Figure 4, we assume as an example that all measurements were actually made to the left side of the fireball. As noted above, the correct solution for this case is obtained by using a negative sign for all of the terms T and U described above, which we designate “L L L“ in the figure legend and in Table 1.

In Figure 4 we show all of the solutions that would be calculated for the hypocenter location for various combinations of the sides that we might assume were measured at each location. Although it is clear that the correct combination, “L L L,” is tangent to all three rays, it also appears that the combination “R R L,” i.e., the solution based on the assumption that the first two locations were measured to the right side of the fireball and the third to the left, is tangent to all three rays. In fact, “R R L“ is actually not quite a perfect fit, but the difference is too small to be visually apparent on this plot. This ambiguity arises because the first and second points are not well separated in terms of their angular distribution about the hypocenter. This problem should not arise in the applications of interest, which have larger numbers of observed rays with a much more homogeneous angular distribution. However, it is clear from even this

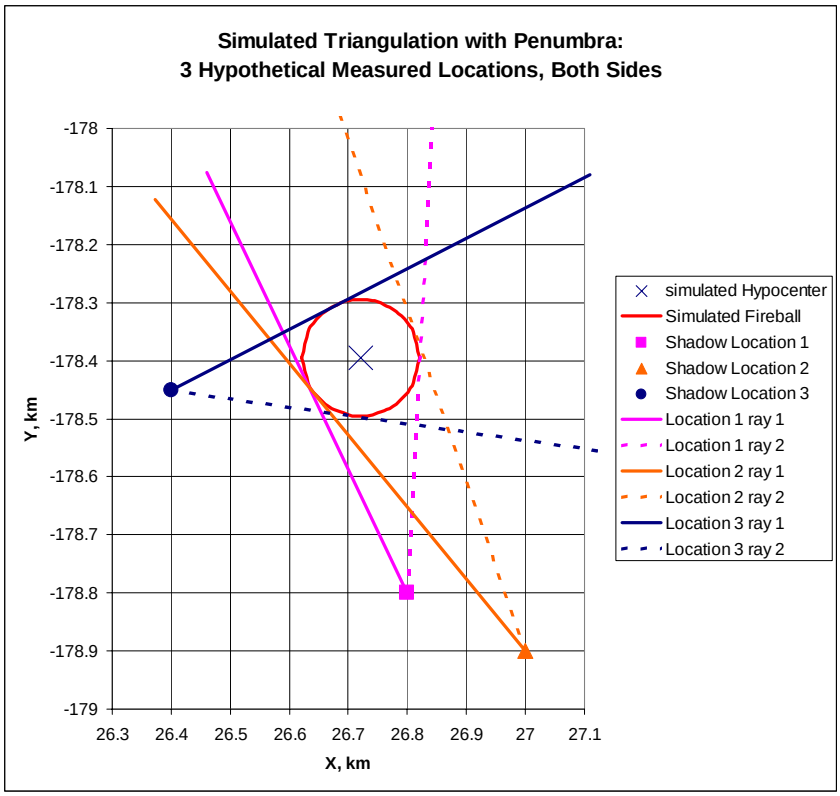

Figure 3. A set of hypothetical locations and the rays that would be measured (without error) to the sides of a 100-m effective fireball radius.

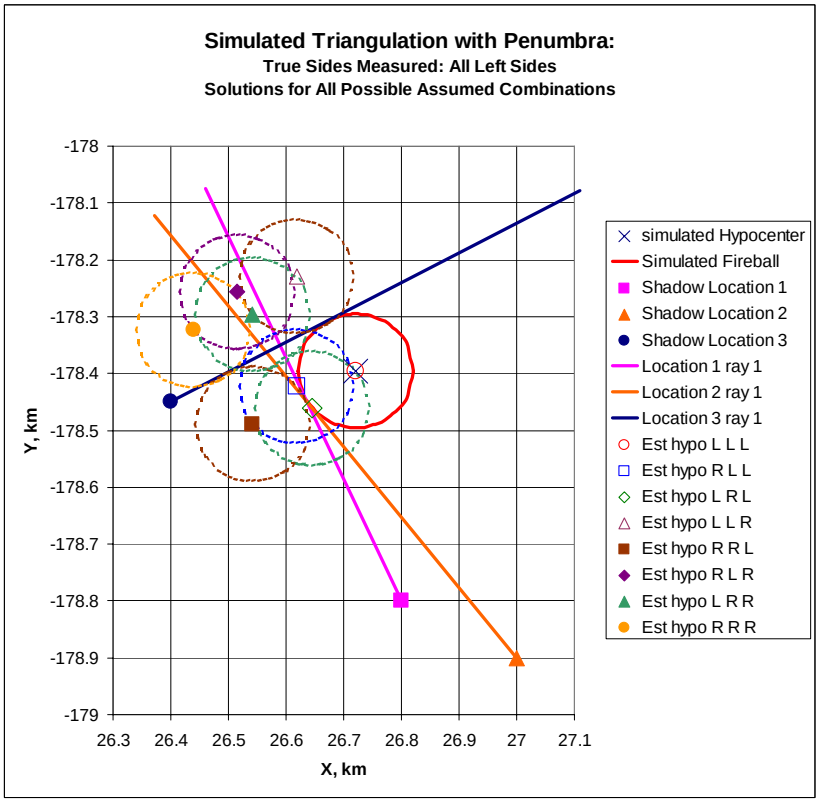

Figure 4. Three measured rays and the hypocenter estimates that would be obtained for all possible combinations of sides assumed to have been measured.

small example that picking a correct combination by visual inspection is impossible, even if errors in the measured angles and coordinates of the measurement sites are negligible and we know the exact size of the effective fireball radius.

In Table 1, we check the sum of squared perpendicular distances in m from the three rays to the fireball for all of the possible combinations of sides assumed to have been measured, for fireball radii in 10-m increments from 10 m to 120 m. That is, for each set of assumptions about the combination of sides measured and the fireball radius, we calculate the minimum sum of squared perpendicular distances, which corresponds to the hypocenter location that we would calculate under those assumptions. In addition to the perfect fit for the the correct combination "L L L," it is notable that the misleading combination "R R L," " fits almost perfectly if the fireball radius is assumed to be 120 m rather than 100 m. It is also apparent from the table that a very small fireball of radius 10 m fits very well for the combination "R L L," although not perfectly. (This possible solution is not shown on the plot in Fig. 4, but it fits into the triangle formed by the intersection of the three measured rays.) Again, such ambiguity should not be encountered in practice if the number of measurements is > 2 and the measurement locations have a reasonably homogeneous distribution of azimuthal angle about the hypocenter.

Now we apply this method to the data of Kanai, shown in Table 2, which include measurements at 14 locations. The locations are well established. They are named in Table 3 of ABCC TR 3-69, along with the authors' estimates of their U.S. Army map coordinates, and they are shown on a reproduction of

Table 1. The minimum sum of squared perpendicular distances for each set of assumptions about the fireball radius and the sides measured.

	Assumed combination of sides measured							
Assumed Fireball radius, m	L L L	L L R	L R L	L R R	R L L	R L R	R R L	R R R
10	266.4	387.7	923.7	1139.8	**6.3**	34.6	275.0	398.0
20	210.5	451.4	1818.8	2438.8	171.9	40.6	225.8	473.7
30	161.2	519.9	3014.3	4226.0	825.7	347.1	181.5	555.9
40	118.4	593.2	4510.2	6501.4	1967.6	953.9	142.0	644.7
50	82.2	671.3	6306.5	9265.1	3597.8	1861.1	107.4	740.1
60	52.6	754.3	8403.2	12516.9	5716.2	3068.7	77.6	842.1
70	29.6	842.1	10800.2	16256.9	8322.8	4576.6	52.6	950.6
80	13.2	934.8	13497.7	20485.1	11417.5	6385.0	32.5	1065.8
90	**3.3**	1032.3	16495.5	25201.6	15000.5	8493.7	17.2	1187.5
100	**0.0**	1134.6	19793.7	30406.2	19071.7	10902.9	**6.7**	1315.8
110	**3.3**	1241.7	23392.3	36099.0	23631.1	13612.4	**1.1**	1450.6
120	13.2	1353.7	27291.3	42280.0	28678.7	16622.3	**0.3**	1592.1

Table 2. The data of Kanai.

Kanai Point No.	Location	GIS-Estimated New City Map Coordinates		Kanai azimuthal angle
		Y, km	X, km	ccw from grid E, deg
1	Branch Office, Sanwa Bank	26.821	-178.485	193
7	Branch, Chiyoda Insurance Co.	26.852	-178.380	221
10	Branch, Sumitomo Bank	26.966	-178.453	194
13	Seiyoken	26.912	-178.656	141
14	Industrial Museum, S side	26.617	-178.317	326
17	Chamber of Commerce and Industry	26.615	-178.182	299
20	Fukuro-machi Primary School	27.035	-178.733	138
23	Hiroshima Central Telephone Bureau	27.136	-178.773	131
24	Branch Office, Yasuda Bank	27.201	-178.614	172
25	Honkawa Primary School	26.357	-178.214	332
29	Chugoku Electric Co.	26.813	-179.085	98
30	Bank of Commerce and Industry Assn	27.337	-178.470	188
35	Hiroshima City Office	26.719	-179.436	454
36	Shin-ohashi Bridge	26.208	-178.725	391

Table 3. Results for Kanai data.

	Best combination for radius		Next to best combination for radius	
Radius, m	**Combination**	**SS, km^2**	**Combination**	**SS, km^2**
10	LRLLLLRRLLLLLL	0.0313	LRLLLLRRLLRLLL	0.0320
20	LRLLLLRRLLLLLL	0.0225	LRLLLLRRLLRLLL	0.0236
30	LRLLLLRRLLLLLL	0.0164	LRLLLLRRLLRLLL	0.0180
40	LLLLLLRRLLLLLL	0.0130	LLLLLLRRLLRLLL	0.0130
50	**LLLLLLRRLLRLLL**	**0.0114**	LRLLLLLRLLLLLL	0.0125
60	LLLLLLRRLLRLLL	0.0120	LRLLLLLRLLLLLL	0.0146
70	LLLLLLRRLLRLLL	0.0150	LLLRLLRRLLRLLL	0.0179
80	LLLLLLRRLLRLLL	0.0202	LLLLLLRRLLRLLR	0.0225
90	LLLRLLRRLLRLRR	0.0225	RRRRLLRRRLLRLL	0.0296
100	LLLRLLRRLLRLRR	0.0226	RRRRLLRRRLLRLL	0.0306

Kanai's original map in Figure 1 of Appendix 3 of ABCC TR 3-69. For this study, the new city map coordinates of these locations were evaluated using the GIS, giving the values in Table 2. This corrects a substantial distortion in the map originally used by Kanai.

The measured azimuthal angles of the shadows are given with respect to magnetic north in Table 3 of ABCC TR 3-69. To restate them with respect to grid east of the newer city maps, we first noted that, according to the declination diagram on the U.S. Army map, magnetic north in Hiroshima in 1945 was 5 deg. 41 min. = 5.683 deg. west of true north. We also calculated from the equations of the Geographical Survey Institute, which relate grid coordinates of the new city map to longitude and latitude in the Tokyo datum (Young and Kerr 2004), that grid north of the new city maps in the Hiroshima area is about 0.2 deg. east of true north. We assumed that the direction "true north" in the Tokyo datum used for the new city maps was the same as "true north" in the datum used for the U.S. Army maps. Thus, to convert from angles specified with respect to 1945 magnetic north to angles specified with respect to new city map grid east, we converted the angles given by Table 3 of ABCC TR 3-69 to angles stated counter clockwise (ccw) from 1945 magnetic north and then added 5.683 + 0.2 + 90 deg. to obtain angles stated ccw from new city map grid east.

The results for the analysis of Kanai's data are given in Table 3. For each effective fireball radius checked, in increments of 10 m, the best and next-best combination of sides measured are shown, along with their sums of squared perpendicular distances. The best combination is for a radius of 50 m and has three sites with measurements to the right side of the fireball and eleven with measurements to the left side of the fireball. This reduces the sum of squares considerably from the assumption of no fireball effect on the measured angles (equivalent to assuming that all of the reported angles were actually for central rays) from 0.0429 km^2 to 0.0114 km^2. The mean absolute perpendicular distance from measured rays to the hypocenter is approximately 47 m for the solution based on the assumption of no fireball effect, whereas the mean absolute perpendicular distance from the measured rays to the effective fireball radius is about 22 m for the best solution with a fireball effect. The hypocenter estimate for the combination **LLLLLLRRLLRLLL** with a 50-m effective fireball radius is at (27.714, -178.465), about 34 m west and 12 m north of the solution for no assumed fireball (equivalent to assuming that all of the reported angles were actually for central rays), which is at (27.748, -178.477). These solutions are shown in relation to the measured rays in Figure 5. The three shadow lines that the optimal fireball-effect solution suggests were measured to the right side of the fireball are shown as dotted lines.

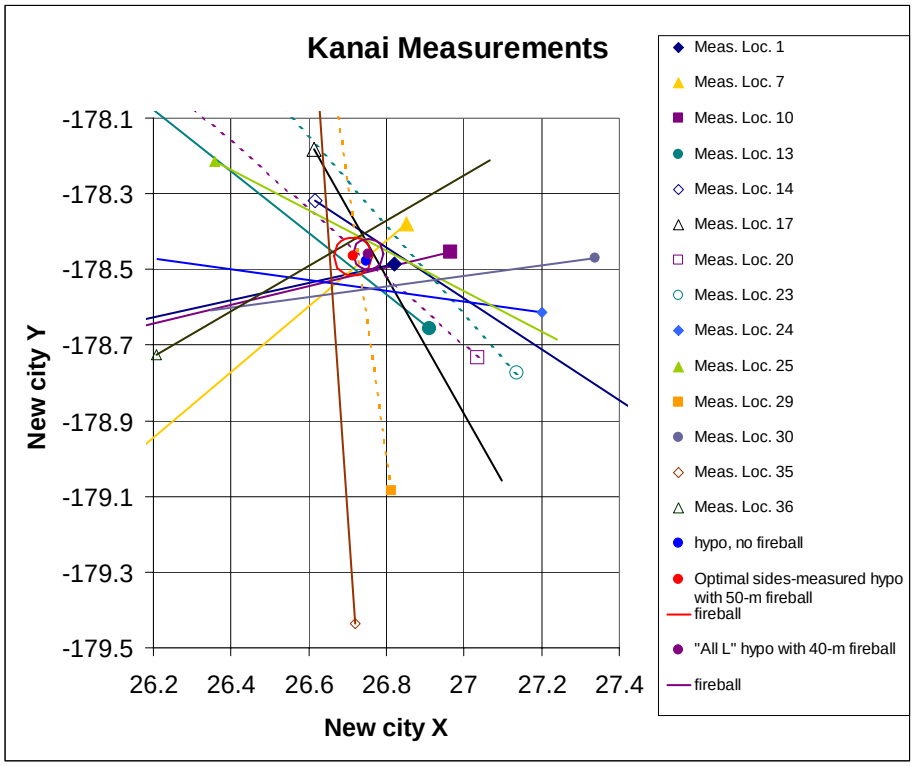

Figure 5. Kanai's measured shadow lines and various possible solutions.

Because the optimal solution suggested that only three shadows were measured to the right side of the fireball, we considered the possibility that all sites were measured to the left side of the fireball, and that the situation of those three lines is due to error. The solution with all measurements to the left of the fireball has a minimum sum of squared perpendicular distances for a radius of 40 m, and its solution is very close to the solution for no fireball effect, as shown in Fig. 5. Its sum of squared perpendicular distances is 0.0274 km^2, and its mean absolute perpendicular distance from the measured rays to the effective fireball radius is about 39 m. This is a small improvement over the assumption of no fireball effect, but not nearly as good as the optimal combination. We also considered the influence of one particular measurement, at location No. 23, the Hiroshima Central Telephone Office. It has the largest error in all of the solutions discussed here, and appears quite discordant with the other lines. However, when this particular observation is omitted, there is little effect on the solutions discussed above. On balance, we feel that the solution for the combination **LLLLLLRRLLRLLL** with a 50-m effective fireball radius is the best one and should be used in the combined estimate. It is also closer to the estimates of the three other major studies than the other two estimates discussed above.

The same method was used to analyze the data of Arakawa and Nagaoka. Those data are more complicated, as many replicate measurements were made at most of the sites measured. The method described above was applied to the *average measured angle for each site*, based on analyses that are too extensive to include here but will be included in a future publication. That is, it appeared from detailed analyses that all of the measurements at a given site were made on the same side of the shadow-casting objects. For example, when the measured angles for each site were plotted, there was no evidence of a bimodal distribution or enough angular separation to suggest that both sides were measured.

As with the Kanai data, the coordinates of the measurement locations were re-evaluated for this study using the GIS. Because a total of 37 sites were measured, it was not practical to exhaustively evaluate all possible combinations of sides measured; however, because the numbers of measurements per site were very unevenly distributed, the vast majority of measurements could be included. The first 16

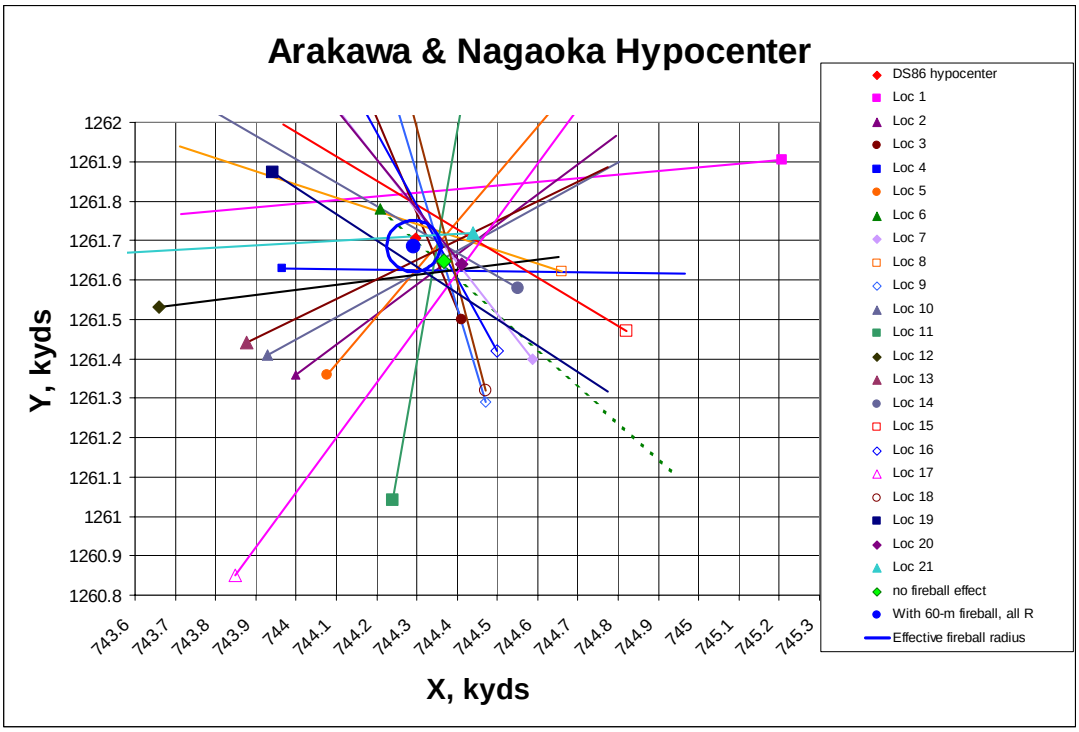

Figure 6. Arakawa and Nagaoka's measured shadow lines and two possible solutions.

sites with the most measurements per site, which include 1104 of the 1178 measurements, were subjected to the full optimization. The optimal solution was for all except one (location No. 6) of the 20 sites being measured to the right side of the fireball. This is clearly seen in Figure 6, in which the shadow line for location No. 6 is shown as a dotted line. For several reasons, we believe it is most plausible that the measurements at this site were actually made to the right of the fireball, and that the result obtained from the optimization is due to the error in the measurements. The difference between the two solutions is small, as the combination chosen here, with all measurements to the right side of the fireball, is at (744.291, 1261.686) in U.S. Army map coordinates, whereas the solution assuming that location No. 6 was measured to the left side of the fireball is at (744.285, 1261.682).

The Measurement Uncertainty Problem

Because of the errors in measured angles and estimates of the coordinates of locations where measurements were made, there is uncertainty in the hypocenter estimate obtained for each set of data, which is related to the quality of the data in that particular study. We need to evaluate this uncertainty quantitatively in order to properly combine the results of studies with different qualities into a single overall estimate of the hypocenter location, as well as to estimate the uncertainty of that combined estimate. There are various ways to approach this problem. One way, which is explored here, is to start with a full probability model of the errors in the input variables and then determine the corresponding error distribution to be expected in the solutions. Another way, which is being considered for future work, is to use a resampling method such as the bootstrap method to evaluate the uncertainty in the solutions.

We do not have ideal information on the uncertainty in the input data for most of the studies, but we do have at least rough estimates of the uncertainty in the measured angles, which were part of what Hubbell *et al* used to weight their overall estimate, and there are some ways to get at least a rough estimate of the accuracy in specifying the coordinates of the measurement locations that investigators would have used in making their original estimates. More importantly, we can give fairly good estimates of the uncertainty in location coordinates for the major studies that are re-analyzed here, because we can relate

them to known sites on the maps and aerial photographs in most cases. In addition, another thing we have for the major studies is the Λ - the sum of squares of perpendicular distances from the measured rays to the solution point constituting the hypocenter estimate. This is a very useful item in view of the insightful observation, as suggested by Hubbell *et al* and undoubtedly others before them, that the size of the Λ must be statistically related to the uncertainty of that estimate. That is, the closer the rays come to converging in a single point at which all of them intersect, the more confidence we can have in the accuracy of the solution.

The approach used here, then, is to seek to establish a statistical relationship between the uncertainty in the input data (x_i, y_i, α_i) of each original study and the uncertainty in both (a) the Λ, and (b) the solution $(\hat{x}, \hat{y})$. The uncertainty in the input data (x_i, y_i, α_i) would be characterized by a fully-specified joint probability density function such as $f(x_i, y_i, \alpha_i; \mu_x, \mu_y, \mu_\alpha, \sigma_x, \sigma_y, \sigma_\alpha)$. Given the form of $f(x_i, y_i, \alpha_i; \mu_x, \mu_y, \mu_\alpha, \sigma_x, \sigma_y, \sigma_\alpha)$, the probability distribution of Λ, which determines its uncertainty, depends on the $\mu_x, \mu_y, \mu_\alpha, \sigma_x, \sigma_y, \sigma_\alpha$ via equation (1) above, and the probability distribution of the hypocenter estimate $(\hat{x}, \hat{y})$ depends on the $\mu_x, \mu_y, \mu_\alpha, \sigma_x, \sigma_y, \sigma_\alpha$ via equation (3) or (19) above, as applicable.

In this work, because of the mathematical difficulty of establishing this relationship in analytical form, we have chosen to use numerical simulation of random errors. We will make simple assumptions about $f(x_i, y_i, \alpha_i; \mu_x, \mu_y, \mu_\alpha, \sigma_x, \sigma_y, \sigma_\alpha)$ and rely on estimating the key relationships by simulatiing of random errors generated from $f(x_i, y_i, \alpha_i; \mu_x, \mu_y, \mu_\alpha, \sigma_x, \sigma_y, \sigma_\alpha)$. We will use this relationship, along with the observed value of Λ and other information available from each original study, to make an estimate of the uncertainty in the input data (x_i, y_i, α_i) of that study. Then we use the same statistical relationship to estimate the uncertainty in the hypocenter estimate for that study. The relationships involved are illustrated in Fig. 7 and are further explained below.

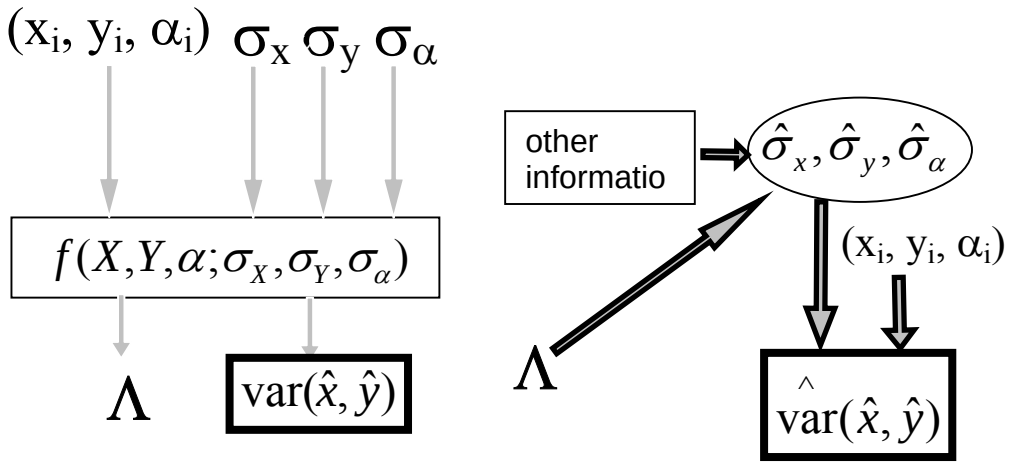

Figure 7. Relationships among quantities involved in estimating the uncertainty of the hypocenter estimates of individual studies.

Uncertainty in Input Values

Measured Angle

The assumption adopted for this work is that the errors in measured angles are *approximately* normally distributed. Clearly this can only be an approximation, because the normal distribution is defined on the entire set of real numbers, from -∞ to +∞, whereas the angles can only extend from -π (-180°) to +π (+180°). But with angle standard deviations on the order of even 10°, about the largest likely to be considered here, the tales of the normal distribution that cannot be accommodated contain infinitesimal mass.

The most complete information, by far, on the reproducibility of measured angles of shadows is given by the data of Arakawa and Nagaoka, as reported in Part I of ABCC TR 12-59. They comprise 1178 measurements, with as many as 219 measurements at a single location. These data thus represent a very important basis for estimating σ_α.

The sample standard deviations of the recorded angles for the 18 sites including the vast majority of the measurements are shown in Table 4, along with the approximate distance of the site from the hypocenter.

Coordinates of Locations Where Measurements Were Made

The locations given by Arakawa and Nagaoka are documented with both specific site names and U.S. Army map coordinates. These could be checked on georeferenced aerial photographs and the new city map for almost all sites, including the 18 sites with the most measurements as shown in Table 4. The data obtained by checking these sites, including consideration of the information given in ABCC TR 3-69 about errors at several of them, is shown in Table 5.

The information on the most measured sites was good enough to specify U.S. Army map coordinates correct to an error standard deviation in each coordinate no more than 15 to 20 m in all cases.

Table 4: Summary data on measured angles of Arakawa and Nagaoka (18 most-measured sites)

Site No.	Ground distance, m	# of observations	sample s.d. of angles measured	estimated s.d. of mean angle for site
1	851	7	1.57	0.59
2	418	181	7.81	0.58
3	215	93	3.08	0.32
4	313	214	6.73	0.73
5	378	35	3.95	0.43
6	105	30	8.74	1.59
7	387	101	3.26	0.60
8	340	39	3.21	0.59
9	412	91	6.32	1.15
10	432	115	6.13	1.12
11	612	14	4.04	0.74
12	605	85	2.52	0.46
13	455	50	6.37	1.16
14	258	18	3.74	0.68
15	524	16	6.77	1.24
16	321	16	3.58	0.65
17	884	11	1.03	0.19
18	387	11	3.89	0.71

Table 5. Measurement locations used by Arakawa and Nagaoka in ABCC TR 12-59

Site No.	Site Name	X	Y	avg angle, deg cw from mag N	deg ccw from Army grid E	rad ccw from grid E
1	Shokaku Temple	745.208	1261.905	259	185.3	3.234
2	Joen Temple	744	1261.36	47	37.3	0.651
3	Sensho Temple	744.41	1261.5	332	112.3	1.960
4	Jisen Temple	743.965	1261.628	85	359.3	6.271
5	Keizo Temple	744.076	1261.358	34	50.3	0.878
6	Sairen Temple	744.21	1261.78	127	317.3	5.538
7	Myoren Temple	744.588	1261.398	317	127.3	2.222
8	Shojun Temple	744.66	1261.62	283	161.3	2.816
9	Kokutai Temple	744.47	1261.29	338	106.3	1.856
10	Myoho Temple	743.93	1261.41	55	29.3	0.512
11	Ryuko Temple	744.24	1261.04	4	80.3	1.402
12	Jokaku Temple	743.66	1261.53	77	7.3	0.128
13	Dempuku Temple	743.877	1261.442	58	26.3	0.459
14	Yasuda Life Insurance Co.	744.55	1261.58	295	149.3	2.606
15	Yasuda Bank	744.82	1261.47	296	148.3	2.589
16	Fukoku Life Insurance Co.	744.5	1261.42	326	118.3	2.065
17	Yorozuyo Bridge	743.85	1260.85	30	54.3	0.948
18	Nippon Bank	744.47	1261.32	340	104.3	1.821
19	Honkawa Grade School	743.941	1261.872	118	326.3	5.695
20	Daiichi Bank	744.41	1261.64	316	128.3	2.240
21	Chiyoda Life Insurance Co.	744.44	1261.72	261	183.3	3.199
22	Gokoku Shrine, outer gate	744.31	1261.91	178	266.3	4.648
23	Kokutai Temple	744.45	1261.17	345	99.3	1.733
24	Seiryu Temple	744.94	1261.6	286	158.3	2.763
25	Sorazaya Shrine	743.96	1262.29	156	288.3	5.032
26	Aioi Bridge, west end	744.02	1261.98	145	299.3	5.224
27	Aioi Bridge, east end	744.12	1261.96	153	291.3	5.084
28	Aioi Bridge, south end	744.05	1261.87	123	321.3	5.608
29	Kiyozumi Temple	743.79	1262.05	126	318.3	5.556
30	Sanwa Bank	744.4	1261.61	335	109.3	1.908
31	Monument (West Parade Ground)	744.5	1261.88	230	214.3	3.741
32	West Reconstruction Board	744.36	1261.9	210	234.3	4.090
33	Bank Club	744.37	1261.52	355	89.3	1.559
34	Nippon Life Insurance Co.	744.38	1261.56	330	114.3	1.995
35	Honkawa Geibi Bank	743.8	1261.63	80	4.3	0.075
36	Osaka Bank	744.57	1261.64	286	158.3	2.763
37	Court	744.94	1261.05	320	124.3	2.170

Results of Random Error Simulation

A number of plots like the one shown in Figure 8, for various assumed error s.d.'s in the measurement location coordinates, were generated by random error simulation and evaluated. The observed standard deviation of the perpendicular distances from the measured rays to the hypocenter estimate noted above, 16.8 m, is shown as a horizontal line in red. Based on the trend in the simulated s.d. of the same quantity, as shown by the triangles on the plot, it was decided to assign error s.d.'s of 2.3 deg and 10 m, respectively, for measured angle and measurement location coordinates, which are quite consistent with the information from other sources noted above.

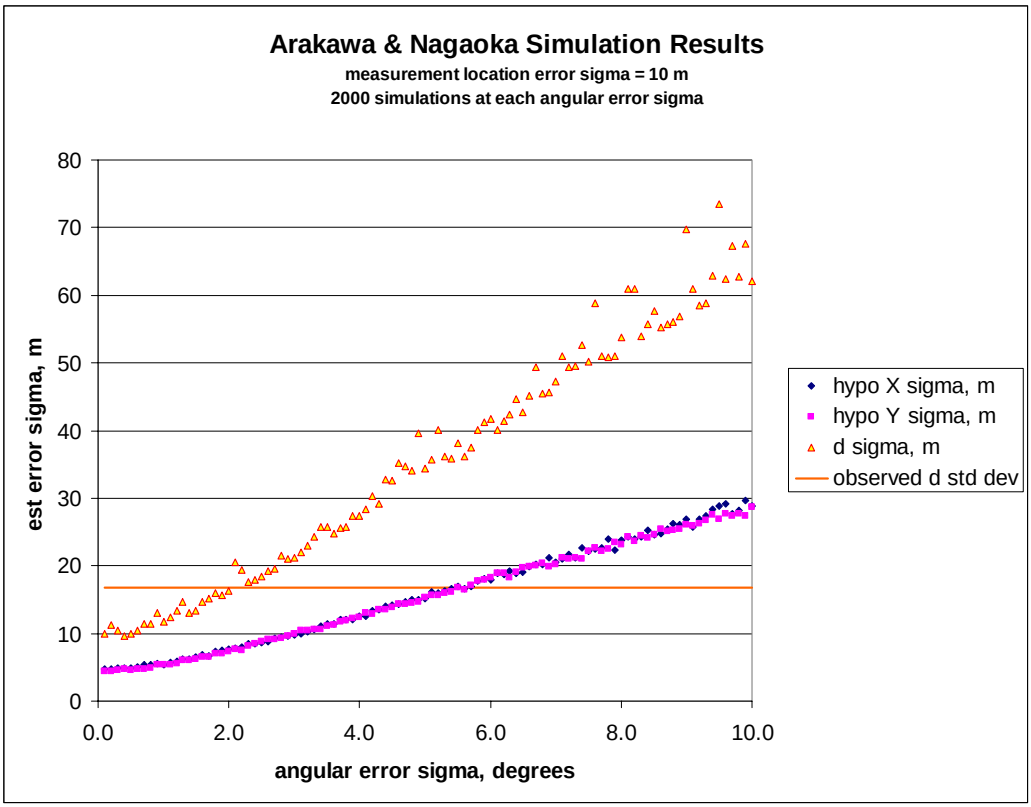

Figure 8. Results of random error simulation for the data of Arakawa and Nagaoka.

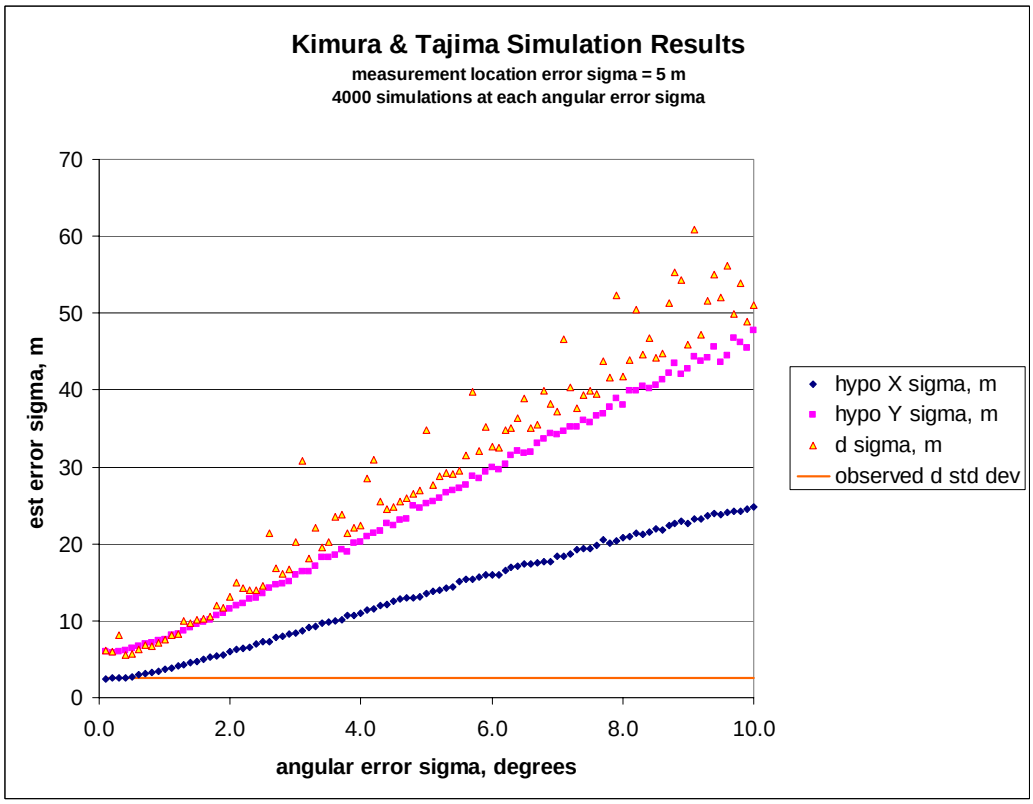

Figure 9. Simulation results for the data of Kimura and Tajima.

One of the virtues of random error simulation as used here is that it includes the effect of asymmetrical angular dispersion of measurement locations about the presumed solution. The uncertainties for the two coordinates of the hypocenter, shown as diamonds and squares in Fig. 8, are virtually identical

because of the relative radial symmetry of the angular dispersion of measurement locations. Even though there are no locations directly north of the hypocenter area in Arakawa and Nagaoka's data, as shown in Fig. 7, there is enough coverage of radial angles to avoid asymmetry in the coordinate uncertainty. On the other hand, the simulation results for the measurement locations of Kimura and Tajima, shown in Figure 9, reflect the fact that there were relatively few measurement locations, as shown in Figure 10, and most of them were north or south of the hypocenter area, so that the uncertainty in the Y coordinate is greater because there is less angular difference for a unit difference in hypocenter location on the Y axis than on the X axis. (The observations shown as dotted arrows entering the diagram from outside its depicted area were not used because they appeared inconsistent with the reported result of Kimura and Tajima when the named measurement locations were evaluated with the GIS, and in the case of the "Gas Tank," the location was unknown.)

The most important unsolved problem in this regard has to do with the numerous small studies included by the authors of ABCC TR 3-69 in their tabulation and their resulting estimates, which they estimated to have only three measurement locations. They have no real documentation of these studies except for their resulting hypocenter estimates. Most importantly, they have no documentation of the locations measured. Simulations to date have indicated that, even when very favorable constraints are imposed on a random selection of measurement locations to avoid any two of them being close to having the same direction from the simulated hypocenter, modest-sized error standard deviations in the simulated errors of the measured angles result in very large errors in the hypocenter estimate with non-negligible probability: the empirical distribution of the simulated errors has "heavy upper tail." As a result, the simulation estimates of the uncertainty in the hypocenter estimates of such studies are unstable, even at

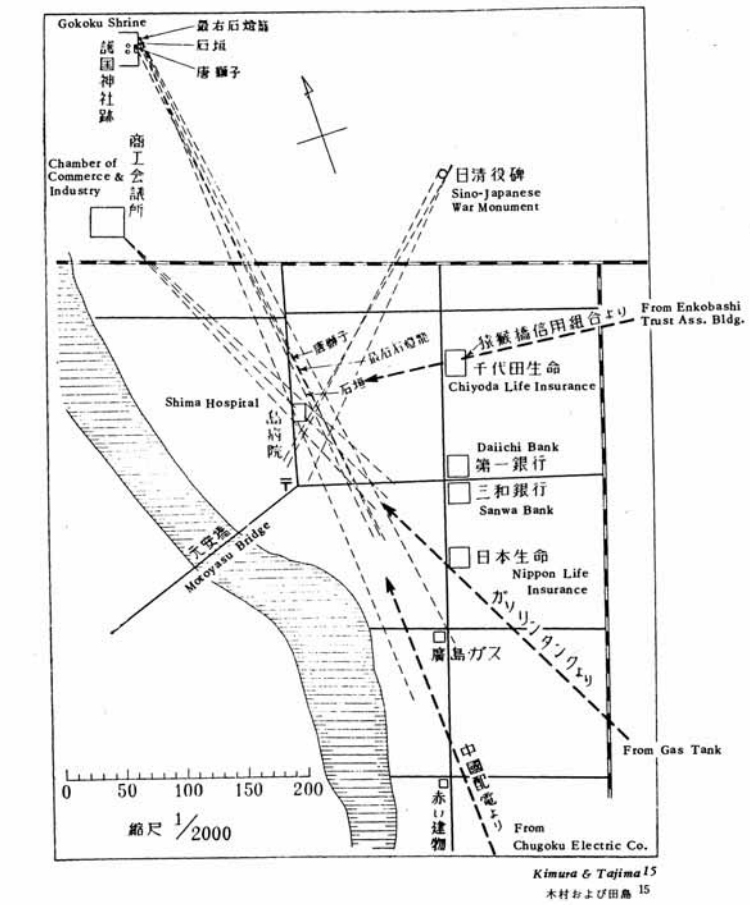

Figure 10. The measurement locations of Kimura and Tajima, from ABCC TR 3-69.

surprisingly large numbers of trials. Although very large number of trials and additional work on simulation may improve the related estimates of uncertainty for such three-location studies, this is an area that requires more statistical research if these small studies are to be considered.

The Statistical Weighting Problem

Although the authors of ABCC TR 3-69 gave tabulated values of estimated error standard deviations in the coordinates for the locations where measurements were made, for all of the individual studies in their Table 1, they did not use them in their weighting for combining the results of those individual studies. They chose instead to estimate the sample standard deviation of the d_i's (perpendicular distances from measured rays to hypocenter estimate) for the various studies, in combination with the estimated standard deviation of the measured angles. They were able to calculate this quantity for the four major studies, but they generally had no quantitative basis for estimating it for the studies lacking recorded measurement data. (They quote a value for the USSBS study that is not footnoted as "Assumed by the present authors," as are the values given in their Table 1 for other studies without measurement data, but they do not provide a source or a basis for this estimate.) Thus, for studies lacking the original data, they based their weights partly on a quantity that depends on the uncertainties in the measured data in a rather complicated way, which they did not determine, and partly on the uncertainties of the measured data themselves. They wrote their formula for weights as $w_i = \frac{\sqrt{N_i}}{\sigma_i \Delta\theta_i}$, where N_i is the number of measurements in the i^{th} study, σ_i is an estimate of the standard deviation of the d_j's of the i^{th} study, and $\Delta\theta_i$ is an estimate of the error standard deviations in the measured angles of the i^{th} study. No statistical derivation is given, and this formula illogically combines uncertainties in an input variable with an uncertainty in an intermediate variable that is influenced by that input variable.

A better and much more obvious method is to estimate the hypocenter coordinates X and Y using weighted sums of the individual study results, with the weights being the inverses of the estimated variances of the X and Y coordinates of the individual estimates, i.e.,

$$\hat{x} = \frac{\sum_{j=i}^{N} w_{x_j} \hat{x}_j}{\sum_{j=1}^{N} w_{x_j}}, \hat{y} = \frac{\sum_{j=i}^{N} w_{y_j} \hat{y}_j}{\sum_{j=1}^{N} w_{y_j}}; \quad w_{xj} = \frac{1}{\hat{\sigma}^2(x)_j}, w_{y_j} = \frac{1}{\hat{\sigma}^2(y)_j} \qquad (26).$$

This is a component-wise application of a standard statistical method used for weighted means of scalar quantities, as suggested by Land in Appendix 1 of ABCC TR 3-69 and in many other texts and references such as, e.g., Bevington and Robinson's popular book *Data Reduction and Error Analysis for the Physical Sciences* (Bevington and Robinson 1992). As Kerr and Solomon observed in their report on the Nagasaki hypocenter, if $\hat{\sigma}_{x_j} = \hat{\sigma}_{y_j} \ \forall j \in 1,...,N$, it is equivalent to minimizing the weighted sum of squares of the Euclidean distances from the combined estimate to the individual estimates, but this method further corrects for situations in which this equality does not apply. Because the $\hat{\sigma}_{x_j}$ *and* $\hat{\sigma}_{y_j}$ are based on all relevant parameters of the individual studies, there is no weighting at this level by the numbers of measurements in each study.

One potential shortcoming of this method is that it does not consider possible covariance between errors in the X and Y coordinates of the hypocenter estimates of individual studies. Thus, it may be necessary to adjust the formulae for covariance.

These methods were used to re-evaluate the hypocenter estimates of the four major studies used in ABCC TR 3-69, and to produce rough preliminary estimates of the uncertainties in all of the individual

study results considered in that report. The results are given in Table 6 and Figure 11. The listing suggested by Land in Appendix 1 to ABCC TR 3-69 is used here to avoid the redundancies in the more complete listing given in that report by Hubbell, Jones, and Cheka.

Table 6. Estimates of hypocenter location for individual studies and combined result.

No. in Hubbell *et al.* Table 1	Source	No. of points measured	Angular error s.d. est from TR 3-69, deg	Angular error s.d. est this work, deg	Assumed error s.d. of coord's of meas. loc's	hypo X	hypo Y	Estimated s.d. of error in hypo X, m	Estimated s.d. of error in hypo Y, m
2	Kure Naval Base Team	3	3	4	25	26.639	-178.334	60	60
3	Arakatsu	3	3	4	25	26.639	-178.334	60	60
4	Watanabe et al	3	3	4	25	26.645	-178.414	60	60
5	Kimura & Tajima	7	1	2	15	26.731	-178.393	9	19
7	Kanai	14	1	5.5	15	26.714	-178.465	25	16.5
10	Tanaka	5	1	2	25	26.736	-178.412	25	25
11	Manhattan Engr District	5	1	2	20	26.639	-178.334	22	22
13	"British" quoted by USSBS	5	1	2	25	26.753	-178.42	25	25
14	Oughterson-Warren Report	5	1	2	25	26.722	-178.356	25	25
16	USSBS	6	1	2	20	26.682	-178.405	20	20
17	US Navy Bureau of Yards & Docks	5	1	2	20	26.761	-178.419	22	22
18	Woodbury & Mizuki	7	1	5.5	15	26.715	-178.418	19	20
20	First ABCC Hypocenter, Wright & Brewer	5	1	2	25	26.675	-178.339	25	25
22	Arakawa & Nagaoka	37	5	2.3	10	26.716	-178.415	8.3	8.3
	Hypo-center estimate				variance of weighted mean, km2			4.21E-05	7.59E-05
	This work	26.716	-178.407		standard deviation of wtd mean, km			0.00649	0.008711
	4 main studies only	26.722	-178.421						
					standard deviation of wtd mean, m			6.489517	8.711441

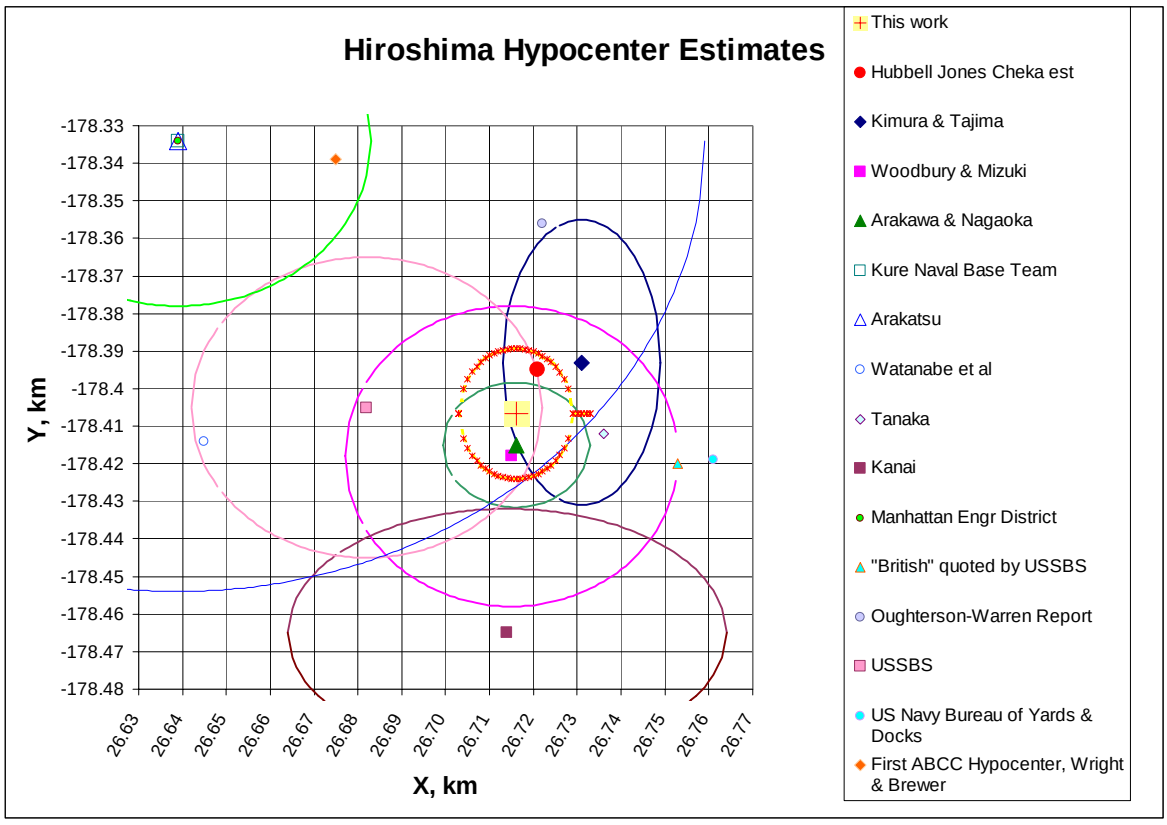

Figure 11. Estimates of individual studies and combined result. Confidence ellipses depicted are 2σ.

As may be seen in Figure 11, there is a remarkable concordance between the results obtained by the methods used here for the reanalysis of the data of Arakawa and Nagaoka and those of Woodbury and Mizuki. Both are somewhat south and west of the result of Kimura and Tajima, and somewhat south of the combined estimate of Hubbell *et al.* as given in ABCC TR 3-69 (1969). Kanai's data remain somewhat apart, despite many efforts, beyond what are described in this work, to investigate possible sources of error, but it is certainly not established that they represent a statistical outlier. Many of the smaller studies shown here are subject to the consideration that, in addition to their large estimated uncertainty based on the initial application of the methods suggested here, their results were specified only very inexactly and were never intended to be used in an effort such as the present work. Although additional work would certainly refine the estimate shown here, it seems likely that the methods and philosophy suggested in this work would result in an estimate generally south of the estimate of Hubbell *et al.*, by a few meters to a few tens of meters.

Conclusions

- Modern computationally intensive methods allow new and better solutions to the problems of interpreting the original measurement data on the location of the Hiroshima hypocenter, with regard to
    - the penumbra problem, and
    - the estimation of the uncertainty in the coordinates resulting from studies for which the measured angles and locations are recorded.
- More statistical research is needed to determine the uncertainty of the results of very small (i.e., about three measured locations) studies with undocumented locations and angles, and to decide what weight, if any, should be given to such results in a combined analysis.
- The method of statistical weighting originally suggested by Land in Appendix 1 of ABCC TR 3-69 is a preferable one and should be used in making combined estimates of the hypocenter location based on the results of various studies.
- Initial results as shown here suggest that estimates of the Hiroshima hypocenter location should be generally south of the location given by Hubbell, Jones, and Cheka in ABCC TR 3-69, by roughly 10 to 25 m.

References

Arakawa ET, Nagaoka S. Determination of the Burst Point and Hypocenter of the Atomic Bomb in Hiroshima. Hiroshima, Japan: Atomic Bomb Casualty Commission; 12-59, Part I; 12-59, Part I; 1959.

Bevington PR, Robinson DK. Data Reduction and Error Analysis for the Physical Sciences. Second ed. New York, NY: WCB McGraw-Hill; 1992.

Draper NR, Smith H. Applied Regression Analysis. Second Edition ed. New York, NY: John Wiley & Sons; 1981.

Hubbell HH, Jr., Jones TD, Cheka JS. The Epicenters of the Atomic Bombs: Reevaluation of All Available Physical Data with Recommended Values. Hiroshima and Nagasaki, Japan: Atomic Bomb Casualty Commission; 3-69; 3-69; 1969.

RERF. US-Japan Joint Reassessment of Atomic Bomb Radiation Dosimetry in Hiroshima and Nagasaki: Final Report. Hiroshima: Radiation Effects Research Foundation; 1987.

Woodbury LA, Mizuki M. Determination of the Burst Point and Hypocenter of the Atomic Bomb in Hiroshima. Hiroshima, Japan: Atomic Bomb Casualty Commission; 12-59, Part II; 12-59, Part II; 1959.

Young RW, Kerr GD. Report of the Joint U.S.-Japan Working Group on Dosimetry, Reassessment of the Atomic Bomb Radiation Dosimetry for Hiroshima and Nagasaki - DS02. Hiroshima: RERF.